

Exactly solvable models for non-Hermitian systems under nonadiabatic quench dynamics

Kangyi Hu(胡康溢), Menghua Deng(邓孟华), and Fuxiang Li(李福祥)

Citation: Chin. Phys. B, 2025, 34 (**5**): 050204. DOI: 10.1088/1674-1056/adbd26
Journal homepage: http://cpb.iphy.ac.cn; http://iopscience.iop.org/cpb

What follows is a list of articles you may be interested in

Study and application of solitary wave propagation at fractional order of time based on SPH method

Luyang Ma(马璐阳), Rahmatjan Imin(热合买提江·依明), and Azhar Halik(艾孜海尔·哈力克)
Chin. Phys. B, 2025, 34 (**5**): 050202. DOI: 10.1088/1674-1056/adbd2a

Dynamic analysis of major public health emergency transmission considering the dual-layer coupling of community-resident complex networks

Peng Yang(杨鹏), Ruguo Fan(范如国), Yibo Wang(王奕博), and Yingqing Zhang(张应青)
Chin. Phys. B, 2024, 33 (**7**): 070206. DOI: 10.1088/1674-1056/ad39c7

Adaptive multi-step piecewise interpolation reproducing kernel method for solving the nonlinear time-fractional partial differential equation arising from financial economics

Ming-Jing Du(杜明婧), Bao-Jun Sun(孙宝军), and Ge Kai(凯歌)
Chin. Phys. B, 2023, 32 (**3**): 030202. DOI: 10.1088/1674-1056/ac9368

Gauss quadrature based finite temperature Lanczos method

Jian Li(李健) and Hai-Qing Lin(林海青)
Chin. Phys. B, 2022, 31 (**5**): 050203. DOI: 10.1088/1674-1056/ac5986

Revealing Chern number from quantum metric

Anwei Zhang(张安伟)
Chin. Phys. B, 2022, 31 (**4**): 040201. DOI: 10.1088/1674-1056/ac2f2c

---

Exactly solvable models for non-Hermitian systems under nonadiabatic quench dynamics

Kangyi Hu(胡康溢), Menghua Deng(邓孟华), and Fuxiang Li(李福祥)†

School of Physics and Electronics, Hunan University, Changsha 410082, *China*

(Received 30 November 2024; revised manuscript received 22 January 2025; accepted manuscript online 6 March 2025)

Due to the nonunitary time evolution and possibly complex energy eigenvalues in non-Hermitian systems, it is still under debate how to properly deal with the dynamics of time-dependent non-Hermitian Hamiltonian. Recently a quantum metric framework has been proposed to study the dynamics of generated defects of a non-Hermitian system under linear quench. Here, we provide an explicit expression for the endowed Hamiltonian under quantum metric for a general two-level non-Hermitian system. Then we propose two exactly solvable models for the study of nonadiabatic dynamics of non-Hermitian systems, and analyze the defect production using the metric method. We find that, in contrast to the direct normalization method, the metric method can reproduce the symmetry of generated defects. The power-law scaling of generated defects with respect to quench time is also obtained.

Keywords: quantum metric, non-Hermitian, quench, non-adiabatic

PACS: 02.60.–x, 02.60.Jh, 03.65.–w, 33.50.Hv

DOI: 10.1088/1674-1056/adbd26 **CSTR:** 32038.14.CPB.adbd26

1. Introduction

Going beyond the conventional Hermitian physics, non-Hermitian physics has attracted enormous interests in diverse areas such as electronic systems,[1–3] classical systems,[4–6] and open quantum systems.[7,8] In non-Hermitian systems, many intriguing physics and interesting phenomena have been unveiled, such as exceptional points,[9–11] non-Hermitian skin effect,[12,13] tachyonic physics,[14,15] and anomoulous bulk-edge correspondence.[16–22] Recently, the research in non-Hermitian physics has also been generalized to non-equilibrium systems.[23–34]

In contrast to the Hermitian systems with real eigenvalues and orthogonal eigenstates, for a general non-Hermitian Hamiltonian, the eigenvalues are not necessarily real and the eigenstates are not orthogonal.[35] With time evolving, the amplitude of the wavefunction would be exponentially increasing or decreasing depending on the sign of the imaginary part of the eigenenergy. Nonorthogonality of eigenvectors also makes invalid the conventional concepts of transition probability in Hermitian quantum mechanics. Therefore, one has to reexamine the whole formalism of Hermitian quantum mechanics, and develop a new theoretical framework for the dynamics of non-hermitian systems.

Different approaches have been adopted to study the dynamics of non-Hermitian systems. The most direct way to deal with the exponentially increasing amplitude of wavevector is to take the explicit normalization of the time-dependent probabilities and observables. This approach has been frequently applied in the open quantum systems,[36–41] but it fails to capture some essential aspects of the physics. A second approach is the biorthogonal quantum mechanics, in which one needs to define an associated state to reformulate the transition probability.[42] This approach has been applied to the study of biorthogonal dynamical quantum phase transition when the non-Hermitian system undergoes a sudden quench.[43] A third approach is provided by the quantum metric framework, wherein the Hilbert space is non-stationary and endowed with a nontrivial time-dependent metric.[44,45] This approach has been shown to be able to recover fundamental theorems of quantum information, and plays a vital role in the violation of quantum adiabaticity when exceptional points are traversed adiabatically. This approach preserves the norm of the wavefunction and thus keeps the notion of probability and the values of observables in a more physical way. However, in the calculation based on the metric framework, the explicit form of the Hamiltonian in the endowed Hilbert space is too complicated, and the underling physics is obscured. More exactly solvable models are needed to enable people to fully understand the approach.

In this paper, we provide an explicit expression for the endowed Hamiltonian under quantum metric for a general two-level non-Hermitian system. The expression of the endowed Hamiltonian has a clear physical meaning. We further propose two exactly solvable models of time-dependent non-Hermitian Hamiltonian, and study the nonadiabatic dynamics and the defect production. Our exactly solvable models predict that the symmetry of the generated defect is recovered, in contrast to the normalization method in which the symmetry of the defect

†Corresponding author. E-mail: fuxiangli@hnu.edu.cn

© 2025 Chinese Physical Society and IOP Publishing Ltd. All rights, including for text and data mining, AI training, and similar technologies, are reserved.

is broken. Moreover, we also obtain the power-law scaling of generated defects with respect to quench time.

2. Metric framwork

We first review the quantum metric framework in the study of non-Hermitian physics.[44,45] One starts from an explicitly time-dependent Hamiltonian $H(t)$, and the corresponding Schrödinger equation

$$\mathrm{i}\frac{\mathrm{d}}{\mathrm{d}t}|\psi(t)\rangle = H(t)|\psi(t)\rangle. \tag{1}$$

The metric framework consists of a dynamical Hilbert space $\mathscr{H}_\rho$ endowed with a positive-definite operator $\rho(t)$, which act as a weight factor in the inner product of this Hilbert space as $\langle\cdot,\cdot\rangle_\rho = \langle\cdot,\rho(t)\cdot\rangle$. The dynamics of the Hilbert space $\mathscr{H}_\rho(t)$ is encoded in the time evolution of the metric $\rho(t)$, given by

$$\mathrm{i}\partial_t\rho = H^\dagger(t)\rho(t) - \rho(t)H(t). \tag{2}$$

After solving the time-dependent metric operator $\rho(t)$, we can map the system to a new Hilbert space $\mathscr{H}$ described by the Hermitian Hamiltonian

$$h(t) = \eta(t)H(t)\eta(t)^{-1} + \mathrm{i}\dot{\eta}(t)\eta(t)^{-1}, \tag{3}$$

where we have introduced the square-root decomposition of the metric, $\rho(t) = \eta^\dagger(t)\eta(t)$.

In the new Hilber space $\mathscr{H}$, the time-evolved state is given by

$$\mathrm{i}\frac{\mathrm{d}}{\mathrm{d}t}|\Psi(t)\rangle = h(t)|\Psi(t)\rangle. \tag{4}$$

Here, the wavevector $|\Psi(t)\rangle$ is related to $|\psi(t)\rangle$ by $|\Psi(t)\rangle = \eta(t)|\psi(t)\rangle$. Note that the construction of $\rho(t)$ guarantees that $h(t)$ is Hermitian, and therefore, the evolution of $|\Psi(t)\rangle$ is unitary at all times, *i.e.*, $\langle\Psi(t)|\Psi(t)\rangle = \langle\psi(t)|\rho(t)|\psi(t)\rangle = 1$. Moreover, this framework also provides a physically meaningful time-dependent expectation value. For an operator $\hat{o}$ in the Hilbert space $\mathscr{H}$, one can define a corresponding operator in the Hilbert space $\mathscr{H}_\rho(t)$ by $\hat{O} = \eta^{-1}(t)\hat{o}\eta(t)$, and the expectation value is given by

$$\langle O(t)\rangle = \langle\Psi(t)|\hat{o}|\Psi(t)\rangle = \langle\psi(t)|\rho(t)\hat{O}|\psi(t)\rangle. \tag{5}$$

Note that the non-Hermitian Hamiltonian $H(t)$ is not quasi-Hermitian and therefore not observable according to traditional quantum mechanics. Instead, the operator

$$\tilde{H}(t) = \eta^{-1}(t)h(t)\eta(t) = H + \mathrm{i}\hbar\eta^{-1}(t)\partial_t\eta(t) \tag{6}$$

is quasi-Hermitian and can be interpreted as the physical operator that plays the role of the energy in the non-Hermitian system.

The most important thing in the metric framework is to determine the expression of $h(t)$ and $\rho(t)$. In this paper, we provide a new and useful expression of $h(t)$ for general two-level non-Hermitian system. For this purpose, one needs to first determine $\eta(t)$ and $\rho(t)$. The explicit derivation of metric $\rho(t)$ in different systems is still an going research.[46–49] A natural choice of $\rho(t)$ is that when the non-Hermitian contribution to the Hamiltonian vanishes, $\rho(t)$ reduces to identity matrix. For a two-level system, the metric $\rho(t)$ can always be written in terms of Pauli matrices

$$\rho = \rho_0\sigma_0 + \boldsymbol{\rho}\cdot\boldsymbol{\sigma}, \tag{7}$$

where $\boldsymbol{\rho} = (\rho_1,\rho_2,\rho_3)$, σ_0 is the identity matric of dimension 2, and $\boldsymbol{\sigma} \equiv (\sigma_x,\sigma_y,\sigma_z)$ are three Pauli matrices.

We choose a Hermitian η, so that $\eta^\dagger(t) = \eta(t)$. Now, one has

$$\eta(t) = \frac{\theta(t)}{2}\mathbb{I} + \sum_{j=x,y,z}\frac{\rho_j(t)}{\theta(t)}\sigma_j, \tag{8}$$

where $\theta(t) = \sqrt{\rho_0+|\boldsymbol{\rho}|} + \sqrt{\rho_0-|\boldsymbol{\rho}|}$.

In this paper, we propose a new expression of $h(t)$ containing only the terms of ρ and not the terms of η, whose expression is usually much more complex than ρ as shown in Eq. (8). Using the properties of η, one can actually eliminate the terms containing the time-derivative of $\eta(t)$, and express $h(t)$ as

$$h = \frac{1}{2}(H+H^\dagger) + \frac{1}{4(\rho_0+\sqrt{\rho_0^2-\boldsymbol{\rho}^2})}[\rho, H-H^\dagger]. \tag{9}$$

More details about Eq. (9) are provided in Appendix A. This expression is new and has a clear physical meaning. The first term is simply Hermitian. The non-Hermiticity comes only from the second term, which is the commutation of metric ρ with the non-Hermitian part of H.

3. Exactly solvable models

In this section, we consider two exactly solvable models and show how the metric framework captures the physics of non-Hermitan dynamics and produces the meaningful results for the nonadiabatic excitation. We will first present the models and the dynamics calculated with the direct normalization method, and then compare them with the metric method.

3.1. Linear quench model and results of normalization method

We consider the following time-dependent two-level non-Hermitian Hamiltonian

$$H = \sum_p H_p, \quad H_p = p\sigma_x + \Delta(t)\sigma_y + \mathrm{i}\Delta(t)\sigma_z \tag{10}$$

with $\Delta(t) = \Delta_0 t/\tau$. Here, τ determines the quenching rate. This model has been studied in Ref. [37] using the normalization method and was denoted as the gapless quench. Here

we will briefly review and confirm the results obtained in Ref. [37]. The eigenenergies of Hamiltonian (10) are $E = p$ with instantaneous right eigenvector

$$|\psi_p^{\mathrm{R}}\rangle = \frac{1}{\sqrt{2}}(1,1)^{\mathrm{T}}, \tag{11}$$

and $E = -p$ with the instantaneous right eigenvector

$$|\psi_{-p}^{\mathrm{R}}\rangle = \frac{1}{\sqrt{2}}(1,-1)^{\mathrm{T}} - \frac{1}{\sqrt{2}}\frac{\mathrm{i}\Delta}{p}(1,1)^{\mathrm{T}}. \tag{12}$$

The instantaneous left eigenvectors are, respectively,

$$|\psi_p^{\mathrm{L}}\rangle = \frac{1}{\sqrt{2}}(1,1)^{\mathrm{T}} + \frac{1}{\sqrt{2}}\frac{\mathrm{i}\Delta}{p}(-1,1)^{\mathrm{T}}, \tag{13}$$

$$|\psi_{-p}^{\mathrm{L}}\rangle = \frac{1}{\sqrt{2}}(1,-1)^{\mathrm{T}}. \tag{14}$$

We have the following biorthogonal relation and completeness relations:

$$\langle\psi_p^{\mathrm{L}}|\psi_p^{\mathrm{R}}\rangle = \langle\psi_{-p}^{\mathrm{L}}|\psi_{-p}^{\mathrm{R}}\rangle = 1, \tag{15}$$

$$\langle\psi_p^{\mathrm{L}}|\psi_{-p}^{\mathrm{R}}\rangle = \langle\psi_{-p}^{\mathrm{L}}|\psi_p^{\mathrm{R}}\rangle = 0, \tag{16}$$

$$\sum_{j=p,-p} |\psi_j^{\mathrm{R}}\rangle\langle\psi_j^{\mathrm{L}}| = 1. \tag{17}$$

Note that the eigenvector $|\psi_{-p}^{\mathrm{R}}\rangle$ is normalized according to Eq. (15).

Now we want to solve the time-dependent Shcrödinger equation with Hamiltonian (10). The wavefunction can be written in terms of the two instantaneous eigenvectors

$$|\psi(t)\rangle = c_1(t)|\psi_p^{\mathrm{R}}\rangle + c_2(t)|\psi_{-p}^{\mathrm{R}}\rangle. \tag{18}$$

Inserting the above wavefunction into the Schrödinger equation, and acting the left eigenvectors $\langle\psi_{p,-p}^{\mathrm{L}}|$ on the left side, one obtains two equations for $c_{1,2}$

$$\mathrm{i}\partial_t c_1 + \frac{\Delta_0}{\tau p}c_2 = pc_1, \tag{19}$$

$$\mathrm{i}\partial_t c_2 = -pc_2. \tag{20}$$

To obtain the above two equations, one needs to use these two identities $\langle\psi_p^{\mathrm{L}}|\mathrm{i}\partial_t\psi_{-p}^{\mathrm{R}}\rangle = \Delta_0/\tau p$, and $\langle\psi_{-p}^{\mathrm{L}}|\mathrm{i}\partial_t\psi_{-p}^{\mathrm{R}}\rangle = 0$. The solutions can be readily written down as

$$c_2(t) = \mathrm{e}^{\mathrm{i}pt}c_2(0), \tag{21}$$

$$c_1(t) = \mathrm{i}\frac{\Delta_0}{p^2\tau}\sin(pt)c_2(0) + \mathrm{e}^{-\mathrm{i}pt}c_1(0). \tag{22}$$

Here, $c_1(0)$ and $c_2(0)$ are two parameters that are to be determined by the initial conditions. If the system starts from state $|\psi_p^{\mathrm{R}}(0)\rangle = \frac{1}{\sqrt{2}}(1,1)^{\mathrm{T}}$ (corresponding to the ground state when $p<0$ and $\Delta(t=0)=0$), then $c_1(0)=1$, and $c_2(0)=0$. The system would stay on the state $|\psi_p^{\mathrm{R}}\rangle$ with just an time-evolving phase factor $\mathrm{e}^{-\mathrm{i}pt}$. However, if the system starts from the state $|\psi_p^{\mathrm{R}}(0)\rangle = \frac{1}{\sqrt{2}}(1,-1)^{\mathrm{T}}$ (corresponding to the ground state when $p>0$ and $\Delta(t=0)=0$), then

$$c_2(t) = \mathrm{e}^{\mathrm{i}pt}, \quad c_1(t) = \mathrm{i}\frac{\Delta_0}{p^2\tau}\sin(pt), \tag{23}$$

thus leading to

$$|\psi(t)\rangle = \frac{\mathrm{e}^{\mathrm{i}pt}}{\sqrt{2}}\begin{pmatrix}1\\-1\end{pmatrix} - \frac{\mathrm{e}^{\mathrm{i}pt}}{\sqrt{2}}\frac{\mathrm{i}\Delta}{p}\begin{pmatrix}1\\1\end{pmatrix} + \mathrm{i}\frac{\Delta_0}{p^2\tau}\frac{\sin(pt)}{\sqrt{2}}\begin{pmatrix}1\\1\end{pmatrix}.$$

Figures 1(a) and 1(b) show the evolution of the state on the Bloch sphere. For $\tau\to\infty$ and $p\neq 0$, the last term vanishes and $|\psi(t)\rangle$ reduces to the instantaneous right eigenfunction (12) and the adiabatic theorem seems to hold.

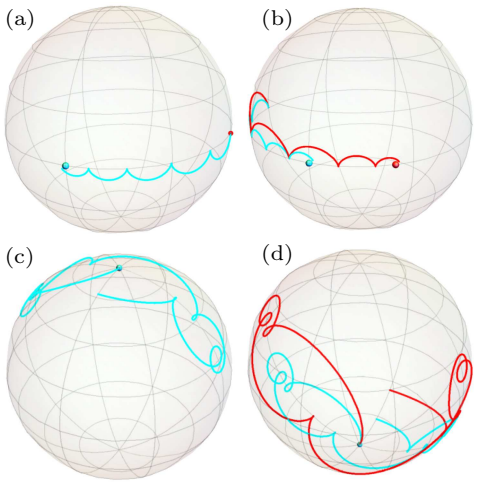


Fig. 1. The evolution of the mapped state $|\Psi(t)\rangle_p = \eta(t)|\psi(t)\rangle_p$ (cyan line) and normalized state $\frac{|\psi(t)\rangle_p}{\langle\psi(t)|\psi(t)\rangle}$(red line) . (a) The case of linear quench when $p<0$. Here $p=-0.5$ and $\tau=30$, the starting point $(1,0,0)$ corresponds to the ground state when $p<0$: $|\Psi(0)\rangle = |\psi(0)\rangle = \frac{1}{\sqrt{2}}(1,1)^{\mathrm{T}}$ and the cyan point represents the ground state of $h(\tau)$ when $p=-0.5$. One can see that the normalized state $|\psi(t)\rangle$ stays at the ground state of $H(t)$ for all time. (b) The case of linear quench when $p>0$. Here $p=0.5$ and $\tau=30$, the starting point for both state is $(-1,0,0)$. The cyan point and the red point correspond to the ground state of $h(\tau)$ and $H(\tau)$ for $p=0.5$, respectively. (c) The case of periodic quench when $p<0$, here $p=-0.75$ and $\omega=0.1$. States evolve from the north pole for both $|\psi\rangle$ and $|\Psi\rangle$, and the gorund state at T is north pole too for both h and H. Note that $|\psi(t)\rangle$ stays at the north pole for all time. (d) The case of periodic quench when $p>0$, here $p=0.75$ and $\omega=0.1$.

Since the norm of the wavefunction is not conserved when time evolution is driven by a non-Hermitian Hamiltonian, an additional prescription for performing measurements in such states has to be given. When interpreting such dynamics as a result of dissipation in the framework of a Lindblad master equation with an additional continuous measurement, expectation values of an operator $\mathcal{O}$ have to be evaluated by taking the normalization of wavefunction[50–52]

$$\langle\mathcal{O}\rangle = \frac{\langle\psi(t)|\mathcal{O}|\psi(t)\rangle}{\langle\psi(t)|\psi(t)\rangle}. \tag{24}$$

The spin expectation is thus given by

$$\langle\sigma_\alpha(p)\rangle_{\mathrm{norm}} = \frac{\langle\psi(t)|\hat{\sigma}_\alpha|\psi(t)\rangle}{\langle\psi(t)|\psi(t)\rangle}. \tag{25}$$

One can explicitly calculate the value of $\langle\sigma_\alpha(p)\rangle_{\rm norm}$ for linear drive model at time $t=\tau$. These results are depicted in Fig. 2 and the explicit expression are presented in Appendix C. One can see that $\langle\sigma_\alpha(p)\rangle_{\rm norm}$ displays no definite parity in the norm computation scheme.

How to properly define the quantity of generated defect is a tricky problem. In Hermitian system, one simply define the probability in the excited states to be the defect after nonadiabatic evolution. In Ref. [37], the authors use the deviation of averaged value of spin operator from its equilibrium value to define the defect, i.e., $\langle\sigma_\alpha^{\rm ex}(p,\tau)\rangle \equiv \langle\sigma_\alpha(p,\tau)\rangle_{\rm norm} - \langle\sigma_\alpha(p,\tau)\rangle_{\rm eq}$. They then integrate the deviation $\langle\sigma_\alpha^{\rm ex}(p,\tau)\rangle$ over p to study the behavior of defect production under nonadiabatic quench dynamics. Here, we also obtain the same scaling behaviors with respect to quench time τ. Explicitly, we obtain $\langle\sigma_{x,y}^{\rm ex}\rangle \sim \tau^{-2}$, and $\langle\sigma_z^{\rm ex}(\tau)\rangle_{\rm norm} \sim \tau^{-1}$. Here, the equilibrium values are

$$\langle\sigma_x(p)\rangle_{\rm eq} = \frac{\Delta_0^2-p^2}{\Delta_0^2+p^2}, \quad \langle\sigma_y(p)\rangle_{\rm eq} = \frac{-2p\Delta_0}{p^2+\Delta_0^2},$$

and $\langle\sigma_z(p)\rangle_{\rm eq}=0$, which are calculated by substituting the right eigenvector (12) into Eq. (25) for $p>0$.

To study the scaling of defect production with respect to quench time τ, one can also study the normalized excitation probability, defined as

$$P_{\rm norm}(p) = \frac{|c_{2(1)}(t)|^2}{|c_1(t)|^2+|c_2(t)|^2}, \tag{26}$$

respectively, for $p>0$ and $p<0$. Actually, this definition is essentially derived from a biorthogonal basis, because $|c_{2(1)}|^2$ represents the proportion of the excited state in the time-evolved state, which is obtained by multiplying the left eigenvector of the biorthogonal state in the time-evolved state. Due to the non-unitary evolution of non-Hermitian system, $|c_1|^2+|c_2|^2\neq 1$, and in order to achieve what is called normalization, all probabilities are divided by a normalized factor $|c_1|^2+|c_2|^2$. Explicit calculation shows that, $P_{\rm norm}(p)=0$ for $p<0$ and

$$P_{\rm norm}(p,\tau) = \Delta_0^2/(\Delta_0^2+p^4\tau^2\csc^2 p\tau) \tag{27}$$

for $p>0$. The behavior of $P_{\rm norm}(p)$ is shown in Fig. 3. One can see that $P_{\rm norm}(p)$ is also highly asymmetric with respect to p. Integrating $P_{\rm norm}(p,\tau)$ over p, one obtains $P_{\rm norm}\sim\tau^{-1/2}$. This result has not been discussed previously.

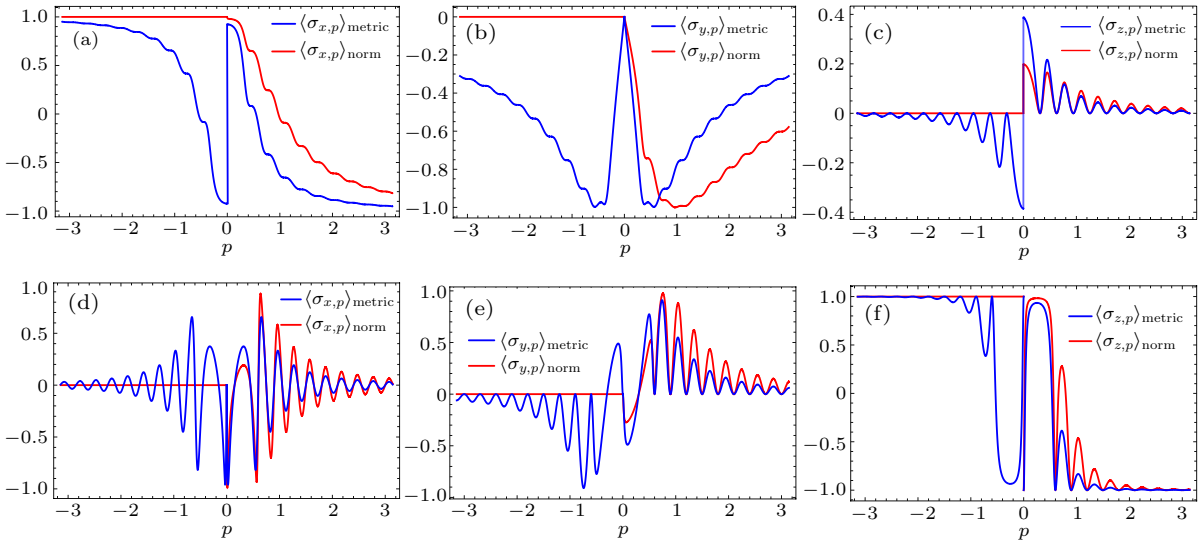


Fig. 2. The expectation values of spin operators obtained from the normalization method and the quantum metric method for the linear quench model [(a)–(c)] and for periodic quench model [(d)–(f)]. Parameters: $\tau=10$, $\omega=0.3$, and $\Gamma_0=\Delta_0=1$.

3.2. Periodic quench model and results of normalization method

Now we introduce a second time-dependent non-Hermitian model to further demonstrate this asymmetry and verify this property. We consider the following Hamiltonian:

$$H_p(t) = p\sigma_z + \Gamma(t)\sigma_x + {\rm i}\Gamma(t)\sigma_y, \tag{28}$$

where $\Gamma(t)=\Gamma_0\sin(2\omega t)$ with $\omega=\pi/T$, and the Hamiltonian evolves from $t=0$ to $t=T$. This model has an advantage that, after one quench cycle, the system returns to its original Hermitian Hamiltonian. Therefore, the excitation probability and the expectation value of operators can be defined in the same way as in Hermitian quantum mechanics.

Denoting $\psi(t)=(a,b)^{\rm T}$, the time-dependent Shcrödinger equation can be explicitly written as

$${\rm i}\partial_t a = pa + 2\Gamma_0\sin 2\omega t b, \tag{29}$$

$${\rm i}\partial_t b = -pb, \tag{30}$$

which can be solved explicitly. The dynamics is still nontrivial as Γ evolves with time even though the energy spectrum is unchanged as $E=\pm|p|$. Starting from the ground state at $t=0$, for $p<0$ the wavefunction only picks up a phase factor

as $e^{-ipt}(1,0)^T$. On the other hand, the $p>0$ ground state at $t=0$ evolves to

$$|\psi(T)\rangle = \begin{pmatrix} \frac{2\Gamma_0\omega}{p^2-\omega^2}\sin(pT) \\ e^{ipT} \end{pmatrix} \tag{31}$$

at $t=T$ and it agrees with the ground state of final Hamiltonian σ_z when $\omega\to 0$. Figures 1(c)–1(d) show the evolution of the state on the Bloch sphere.

Here, we leave the explicit expression in Appendix C, and only discuss the scaling behaviors of the integrated values of spin excitation. One obtains that, $\langle\sigma_x^{\rm ex}\rangle\sim T^{-2}$, $\langle\sigma_{y,z}^{\rm ex}\rangle\sim T^{-1/2}$.

To study the scaling of excitation with respect to quench time T, one can also study the normalized excitation probability. Since the Hamiltonian reduces to Hermitian at final time. The excitation for $p>0$ at $t=T$ is easily defined as

$$P_{\rm norm}(p,T) = \frac{\langle\sigma_z(p)\rangle_{\rm norm}+1}{2} \tag{32}$$

$$= \frac{4\Delta_0^2\omega^2}{4\Delta_0^2\omega^2+(p^2-\omega^2)^2\csc^2(pT)}. \tag{33}$$

The excitation is also highly asymmetric with respect to p, since for $p<0$, $P_{\rm norm}(p,T)=0$. The behavior of $P_{\rm norm}(p)$ is shown in Fig. 3. Integrating $P_{\rm norm}(p,T)$ over p, one obtains $P_{\rm norm}\sim T^{-1/2}$.

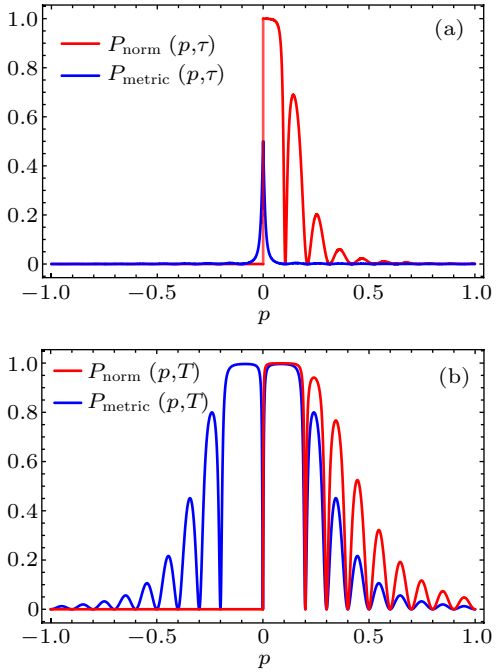


Fig. 3. The momentum-resolved excitation obtained from the normalization method (red) and quantum metric method (blue) for the linear quench model (a) and for periodic quench model (b). Parameters: $\tau=30$, $\omega=0.1$, and $\Gamma_0=\Delta_0=1$.

4. Quantum metric of exactly solvable models

In this section, we will present the results of quantum metric method for the two exactly solvable models, and then compare them with the direct normalization method. We will see that the metric framework captures the physics of non-Hermitan dynamics and produces the meaningful results for the nonadiabatic excitation.

4.1. Linear quench model

We first consider the Hamiltonian (10) driven by $\Delta=\Delta_0 t/\tau$. To solve Eq. (2) for a general non-Hermitian Hamiltonian $H(t)$ of a two-level system, we find two linearly independent solutions to the time-dependent Schrödinger equation

$$i\frac{d}{dt}|\phi_i(t)\rangle = H_p^\dagger(t)|\phi_i(t)\rangle, \tag{34}$$

which describes the dynamics under the Hermitian conjugate, $H_p^\dagger(t)$. The metric $\rho(t)$ is then given by[53]

$$\rho(t) = \sum_{i=1,2}|\phi_i(t)\rangle\langle\phi_i(t)|, \tag{35}$$

which satisfies Eq. (2) by construction. $|\phi_1(t)\rangle$ and $|\phi_2(t)\rangle$ starting from $\frac{1}{\sqrt{2}}(1,1)^T$ and $\frac{1}{\sqrt{2}}(1,-1)^T$ are

$$\begin{aligned}|\phi_1(t)\rangle &= \frac{e^{-ipt}}{\sqrt{2}}\begin{pmatrix}1\\1\end{pmatrix} - \frac{e^{-ipt}}{\sqrt{2}}\frac{i\Delta}{p}\begin{pmatrix}1\\-1\end{pmatrix} \\ &\quad + i\frac{\Delta_0}{p^2\tau}\frac{\sin(pt)}{\sqrt{2}}\begin{pmatrix}1\\-1\end{pmatrix}, \\ |\phi_2(t)\rangle &= e^{ipt}\begin{pmatrix}1\\-1\end{pmatrix}.\end{aligned} \tag{36}$$

Such the choice of the initial condition of $|\phi_i(t)\rangle$ guarantees that $\rho(0)=\mathbb{I}$ which is corresponding to the Hermitian starting point.

The metric $\rho(t)$ can be expressed in terms of Pauli matrices

$$\rho(t) = \rho_0(t)\mathbb{I} + \sum_{j=x,y,z}\rho_j(t)\sigma_j \tag{37}$$

with

$$\begin{aligned}\rho_0(t) &= 1+\frac{\Delta_0^2(1+2p^2t^2-\cos 2pt-2pt\sin 2pt)}{4p^4\tau^2}, \\ \rho_1(t) &= -\frac{\Delta_0^2(1+2p^2t^2-\cos 2pt-2pt\sin 2pt)}{4p^4\tau^2}, \\ \rho_2(t) &= \frac{\Delta_0(2pt-\sin 2pt)}{2p^2\tau}, \\ \rho_3(t) &= -\frac{\Delta_0\sin^2 pt}{p^2\tau}.\end{aligned} \tag{38}$$

Then one can obtain the spin expectation value under metric framework:

$$\langle\sigma_\alpha\rangle_{\rm metric} = \langle\Psi(t)|\hat{\sigma}_\alpha|\Psi(t)\rangle, \tag{39}$$

which can be written explicitly as

$$\langle\sigma_x(p,\tau)\rangle_{\rm metric} = -\left(\frac{4}{\rho_0(\tau)+1}-1\right)\mathrm{sgn}(p), \tag{40}$$

$$\langle\sigma_y(p,\tau)\rangle_{\rm metric} = -\frac{2\rho_2(\tau)}{\rho_0(\tau)+1}\mathrm{sgn}(p), \tag{41}$$

$$\langle\sigma_z(p,\tau)\rangle_{\text{metric}} = -\frac{2\rho_3(\tau)}{\rho_0(\tau)+1}\text{sgn}\,(p). \tag{42}$$

Compared with highly asymmetric $\langle\sigma_\alpha(p)\rangle_{\text{norm}}$ by using the normalization method, $\langle\sigma_\alpha\rangle_{\text{metric}}$ displays a definite parity as shown in Fig. 2. This symmetry structure is a direct consequence of the generalized symmetry discussed in Ref. [54]. In this paper we introduce another explanation as will be discussed later, the parity of $\langle\sigma_\alpha\rangle_{\text{metric}}$ can be deduced by the mapped Hermitian Hamiltonian h since the excitation after metric is always symmetric.

Note that, $\langle\sigma_x(p,\tau)\rangle_{\text{metric}}$ and $\langle\sigma_z(p,\tau)\rangle_{\text{metric}}$ are both odd functions of p, while $\langle\sigma_y(p,\tau)\rangle_{\text{metric}}$ is an even function of p, as illustrated in Fig. 2. Therefore, the averaged values of spin operators $\int\langle\sigma_{x,z}\rangle\,\mathrm{d}p$ are always equal to 0. In this case, one can only calculate the scaling of $\langle\sigma_y(\tau)\rangle_{\text{metric}}$ with respect to τ. Numerically, one obtains a scaling $\langle\sigma_y(\tau)\rangle^{\text{ex}}_{\text{metric}} \sim \tau^{-2}$. Note that the equilibrium value

$$\langle\sigma_y(p,\tau)\rangle_{\text{eq}} = -\frac{4p\Delta_0}{4p^2+\Delta_0^2}\text{sgn}\,(p)$$

needs to be subtracted when integrating $\langle\sigma_y(p,\tau)\rangle_{\text{metric}}$.

Using Eq. (9), we obtain the mapped Hamiltonian

$$\begin{aligned} h_p &= h_x(t)\sigma_x + h_y(t)\sigma_y \\ &= \left(p - \frac{\rho_2\Delta}{\rho_0+1}\right)\sigma_x + \frac{2\Delta}{\rho_0+1}\sigma_y. \end{aligned} \tag{43}$$

The time-dependent wavefunction, as defined in Eq. (4), can be represented in the instantaneous eigenstates $|\Psi(t)\rangle_p = \sum_{n=1,2} c_{n,p}|n(t)\rangle_p$. Here we use $c_1(t)$ to denote the coefficient of the excited state and $c_2(t)$ to that of the ground state. Figures 1(a) and 1(b) show the evolution of the mapped state on the Bloch sphere. Under metric framework, the excitation is defined very well and reads simply

$$\begin{aligned} &P_{\text{metric}}(p,\tau) = |c_1(\tau)|^2 \\ &= \frac{1}{2} - \frac{2p^2(\Delta_0^2+4p^2)\tau^2 + \Delta_0^2\cos(2p\tau) - \Delta_0^2}{2\sqrt{f(p,\tau)}}, \end{aligned} \tag{44}$$

where $f(p,\tau) = \Delta_0^4 - 4\Delta_0^4p^2\tau^2 + 16\Delta_0^2p^4\tau^2 + 4\Delta_0^4p^4\tau^4 + 32\Delta_0^2p^6\tau^4 + 64p^8\tau^4 - 2\Delta_0^4\cos(2p\tau) + 4\Delta_0^4p^2\tau^2\cos(2p\tau) - 16\Delta_0^2p^4\tau^2\cos(2p\tau) + \Delta_0^4\cos(2p\tau)^2$ is even in p. This result is depicted in Fig. 3. Integrating $P_{\text{metric}}(p,\tau)$ over p, one obtains the scaling behavior of $P_{\text{metric}} \sim \tau^{-2}$.

4.2. Periodic quench model

Similarly, the same procedure can be applied to the periodic quench model (28) and the metric operator is

$$\rho(t) = \sum_{i=1,2}|\phi_i(t)\rangle\langle\phi_i(t)|, \tag{45}$$

where $|\phi_1(t)\rangle$ and $|\phi_2(t)\rangle$ starting form $(1,0)^{\text{T}}$ and $(0,1)^{\text{T}}$ are

$$|\phi_1(t)\rangle = \mathrm{e}^{-\mathrm{i}pt}\begin{pmatrix} 1 \\ \frac{\Delta_0(\mathrm{i}\omega\mathrm{e}^{2\mathrm{i}pt} - \mathrm{i}\omega\cos 2\omega t + p\sin 2\omega t)}{p^2-\omega^2} \end{pmatrix}, \tag{46}$$

$$|\phi_2(t)\rangle = \mathrm{e}^{\mathrm{i}pt}\begin{pmatrix} 0 \\ 1 \end{pmatrix}. \tag{47}$$

At the end of the evolution,

$$\begin{aligned} \rho_0(T) &= 1 + \frac{2\Delta_0^2\omega^2}{(p^2-\omega^2)^2}\sin^2(pT), \\ \rho_1(T) &= -\frac{2\Delta_0\omega}{p^2-\omega^2}\sin(pT)\cos(pT), \\ \rho_2(T) &= -\frac{2\Delta_0\omega}{p^2-\omega^2}\sin^2(pT), \\ \rho_3(T) &= -\frac{2\Delta_0^2\omega^2}{p^2-\omega^2}\sin^2(pT). \end{aligned} \tag{48}$$

Then one can obtain $\langle\sigma_\alpha\rangle_{\text{metric}} = \langle\psi(T)|\rho(T)\hat{\sigma}_\alpha|\psi(T)\rangle$. Explicitly, one has

$$\langle\sigma_x(p,T)\rangle_{\text{metric}} = -\frac{2\rho_1(T)}{\rho_0(T)+1}\text{sgn}\,(p), \tag{49}$$

$$\langle\sigma_y(p,T)\rangle_{\text{metric}} = -\frac{2\rho_2(T)}{\rho_0(T)+1}\text{sgn}\,(p), \tag{50}$$

$$\langle\sigma_z(p,T)\rangle_{\text{metric}} = -\left(\frac{4}{\rho_0(T)+1} - 1\right)\text{sgn}\,(p). \tag{51}$$

One can see that $\sigma_x(p,T)$ is even while $\sigma_{y,z}(p,T)$ are odd with p, as depicted in Fig. 2. From Eq. (9) we obtain

$$h(t) = \Gamma\left(1 + \frac{\rho_3}{2(\rho_0+1)}\right)\sigma_x + \left(p - \frac{\Gamma\rho_1}{2(\rho_0+1)}\right)\sigma_z. \tag{52}$$

At final moment one obtains $h_p(T) = H_p(T) = p\sigma_z$, then the momentum resolved excitation is

$$P_{\text{metric}}(p,T) = \frac{\text{sgn}\,(p)\langle\sigma_z(p,T)\rangle_{\text{metric}} + 1}{2} \tag{53}$$

$$= \frac{\Delta_0^2\omega^2}{\Delta_0^2\omega^2 + (p^2-\omega^2)^2\csc^2(p\pi/\omega)}, \tag{54}$$

which is even in p. Figures 1(c) and 1(d) show the evolution of the mapped state on the Bloch sphere. We find that the quantum metric restores the parity of $\langle\sigma_\alpha\rangle$ and the symmetry of the excitation as depicted in Fig. 3. Integrating $P_{\text{metric}}(p,T)$ over p, we obtain $P_{\text{metric}}(T) \sim T^{-1/2}$. All the scaling exponents are summarized in Tables 1 and 2.

Table 1. Scaling exponents α of the averaged spin operators and number excitations which scale as $\tau^{-\alpha}$ with quench time for linear quench model. The exponents are obtained numerically. 'NaN' denotes that there is no scaling, since the quantity is always zero.

Method	$\langle\sigma_x\rangle$	$\langle\sigma_y\rangle$	$\langle\sigma_z\rangle$	P (excitation)
Normalization	1.99	1.98	1.00	0.50
Metric	NaN	1.95	NaN	1.99

Table 2. Scaling exponents α of the averaged spin operators and number excitations which scale as $T^{-\alpha}$ with quench time for periodic quench model. The exponents are obtained numerically.

Method	$\langle\sigma_x\rangle$	$\langle\sigma_y\rangle$	$\langle\sigma_z\rangle$	P (excitation)
Normalization	1.95	0.49	0.49	0.50
Metric	1.96	NaN	NaN	0.50

4.3. Symmetry analysis

From the mapped Hamiltonian (43), considering Eq. (38), one can see that h_x is odd in p while h_y is even, which implies the symmetry $\sigma_y h_p \sigma_y = h_{-p}$. The normalized time-evolved state $|\Psi(t)\rangle_p$ can be represented in the instantaneous eigenstates $|\Psi(t)\rangle_p = \sum_{n=1,2} c_{n,p}|n(t)\rangle_p$. The afore-mentioned symmetry $\sigma_y h_p \sigma_y = h_{-p}$ guarantees that the instantaneous eigenstates satisfy

$$\sigma_y|n(t)\rangle_p \Leftrightarrow |n(t)\rangle_{-p}, \tag{55}$$

which is similar to the consequence induced by unitary transformation operator mentioned in Ref. [54]. To explain the symmetry of the excitation with respect to p, we focus on the evolution of the coefficient

$$\mathrm{i}\partial_t c_{m,p} + \sum_{n=1,2}\langle m_p|\partial_t n\rangle_p = c_{m,p}e_{m,p}, \tag{56}$$

$$\mathrm{i}\partial_t c_{m,-p} + \sum_{n=1,2}\langle m_{-p}|\partial_t n\rangle_{-p} = c_{m,-p}e_{m,-p}, \tag{57}$$

where we omit the time dependence for the ease of notation. Substituting expression (55) together with the even parity of the spectrum $e_p = e_{-p}$ into Eq. (57), and considering the same initial condition for $\pm p$, we can infer that the time-dependent coefficients of the time-evolved state are even in p, i.e., $c_{n,p}(t) = c_{n,-p}(t)$ for all n at all time. The same results can be obtained for h mapped from Eq. (28) through similar process. So we can come to a conclusion that quantum metric restores the symmetry structure of excitation. Thus, from Eq. (44) one can infer that $h_\alpha\langle\sigma_\alpha\rangle$ must hold even parity in p, then the parity of $\langle\sigma_\alpha\rangle_{\text{metric}}$ has to be the same as h_α.

5. Conclusion

In this paper based on two exactly sovable models, we have compared the two approaches, the normalization method and the quantum metric framework, and the different consequences in the nonadiabatic dynamics of non-Hermitian systems. We find that the metric framework recovers the inherent symmetry of spin excitations and number excitations, which has been lost in the normalization method. Moreover, we have further studied the scaling behavior of excitations obtained from the two approaches, and the scaling exponents are the same for most cases if the physical observables are defined properly. Our work paves the way for future studies on the nonadiabatic dynamics of non-Hermitian systems.

Appendix A: Derivtion of the explicit expression of h

For a two-level system, the density matrix can be written in terms of Pauli matrices in the following general form: $\rho = \rho_0\mathbb{I} + \boldsymbol{\rho}\cdot\boldsymbol{\sigma}$, where $\boldsymbol{\rho} = (\rho_1,\rho_2,\rho_3)$. Thus

$$\eta = \frac{\theta}{2} - \frac{\rho_0}{\theta} + \frac{1}{\theta}\rho, \quad \eta^{-1} = \frac{1}{A}\left(\frac{\theta}{2} + \frac{\rho_0}{\theta} - \frac{1}{\theta}\rho\right),$$

where

$$A = \det(\hat{\rho}) = \frac{\theta^2}{4} - \frac{\rho^2}{\theta^2}.$$

Since the Hamiltonian h is Hermitian, we can express h as

$$\frac{h+h^\dagger}{2} = \frac{\eta H\eta^{-1} + \eta^{-1}H\eta}{2} + \frac{[\mathrm{i}\partial_t\eta,\eta^{-1}]}{2}. \tag{A1}$$

For the last term,

$$\begin{aligned}&[\mathrm{i}\partial_t\eta,\eta^{-1}]\\ &= \frac{1}{A}\left[\mathrm{i}\partial_t\left(\frac{\theta}{2} - \frac{\rho_0}{\theta}\right) + \frac{1}{\theta}\mathrm{i}\partial_t\rho - \frac{\theta'}{\theta^2}\rho, \frac{\theta}{2} + \frac{\rho_0}{\theta} - \frac{1}{\theta}\rho\right]\\ &= \frac{1}{A\theta^2}[\mathrm{i}\partial_t\rho, -\rho].\end{aligned}$$

Substituting (2) into the above expression, we get

$$[\mathrm{i}\partial_t\eta,\eta^{-1}] = \frac{1}{A\theta^2}(\rho H^\dagger\rho - \rho^2 H - H^\dagger\rho^2 + \rho H\rho). \tag{A2}$$

Meanwhile, for the first term in Eq. (A1), one has

$$\begin{aligned}&\eta H\eta^{-1} + \eta^{-1}H^\dagger\eta\\ &= \left[\frac{1}{A}\left(\frac{\theta^2}{4} - \frac{\rho_0^2}{\theta^2}\right)H + \left(\frac{\theta}{2} + \frac{\rho_0}{\theta}\right)\frac{1}{\theta}\rho H - \frac{H\rho}{\theta}\left(\frac{\theta}{2} - \frac{\rho_0}{\theta}\right)\right.\\ &\quad - \frac{1}{\theta^2}\rho H\rho + \left(\frac{\theta^2}{4} - \frac{\rho_0^2}{\theta^2}\right)H^\dagger + \left(\frac{\theta}{2} + \frac{\rho_0}{\theta}\right)\frac{H^\dagger\rho}{\theta}\\ &\quad \left. - \frac{\rho H^\dagger}{\theta}\left(\frac{\theta}{2} - \frac{\rho_0}{\theta}\right) - \frac{1}{\theta^2}\rho H^\dagger\rho\right].\end{aligned} \tag{A3}$$

Therefore, totally one arrives at

$$h = \frac{1}{2}(H + H^\dagger) + \frac{1}{4(\rho_0 + \sqrt{\rho_0^2 - \rho^2})}[\rho, H - H^\dagger]. \tag{A4}$$

Appendix B: A Hermitian example

A Hermitian example of time-dependent system with constant eigenenergies is given by

$$H(t) = \varepsilon\cos(2\beta t)\sigma_x + \varepsilon\sin(2\beta t)\sigma_y \tag{B1}$$

with eigenenergies: $E = \pm\varepsilon$, and eigenvectors

$$|\phi_1\rangle = |\psi_+\rangle = \frac{1}{\sqrt{2}}(\mathrm{e}^{-\mathrm{i}\beta t}, \mathrm{e}^{\mathrm{i}\beta t})^{\mathrm{T}}, \tag{B2}$$

$$|\phi_2\rangle = |\psi_-\rangle = \frac{1}{\sqrt{2}}(\mathrm{e}^{-\mathrm{i}\beta t}, -\mathrm{e}^{\mathrm{i}\beta t})^{\mathrm{T}}. \tag{B3}$$

Wave function is a combination of the two eigenstates

$$|\psi(t)\rangle = c_1(t)|\psi_1\rangle + c_2(t)|\psi_2\rangle, \tag{B4}$$

with coefficients satisfying the following equations:

$$\mathrm{i}\partial_t c_1 = \varepsilon c_1 - \beta c_2, \tag{B5}$$

$$\mathrm{i}\partial_t c_2 = -\beta c_1 - \varepsilon c_2. \tag{B6}$$

The solutions are

$$\begin{pmatrix} c_1(t) \\ c_2(t) \end{pmatrix} = a_1 \mathrm{e}^{-\mathrm{i}\lambda t} \begin{pmatrix} \cos(\theta/2) \\ -\sin(\theta/2) \end{pmatrix} + a_2 \mathrm{e}^{\mathrm{i}\lambda t} \begin{pmatrix} \sin(\theta/2) \\ \cos(\theta/2) \end{pmatrix} \tag{B7}$$

with $\lambda = \sqrt{\varepsilon^2+\beta^2}$, and $\tan\theta = -\beta/\varepsilon$.

If we start from $|\psi_2\rangle$, thus $c_2(0)=1$ and $c_1(0)=0$, we have $a_1 = -\sin(\theta/2)$ and $a_2 = \cos(\theta/2)$, and

$$c_1(t) = \mathrm{i}\sin\theta\sin\lambda t, \tag{B8}$$

$$c_2(t) = \cos\lambda t + \mathrm{i}\cos\theta\sin\lambda t. \tag{B9}$$

The excitation is proportional to $|c_1(t)|^2$, which, at the long time limit and adiabatic limit ($\beta \to 0$), scales with β^2/ε^2.

Appendix C: Explicity results of expectation values of spin operators

For the linear quench model, explicit calculation based on normalization method gives rise to the following expressions for expectations of spin operators. For $p<0$, $\langle\sigma_x\rangle = 1$, and $\langle\sigma_y\rangle = \langle\sigma_z\rangle = 0$. For $p>0$,

$$\begin{aligned} \langle\sigma_x(p)\rangle_{\mathrm{norm}} &= 1 - \frac{4p^4\tau^2}{g(p,\tau)}, \\ \langle\sigma_y(p)\rangle_{\mathrm{norm}} &= \frac{2p^2\tau\Delta_0(\sin(2p\tau)-2p\tau)}{g(p,\tau)}, \\ \langle\sigma_z(p)\rangle_{\mathrm{norm}} &= \frac{4p^2\tau\Delta_0\sin^2(p\tau)}{g(p,\tau)} \end{aligned} \tag{C1}$$

with $g(p,\tau) = \Delta_0^2 + 2p^2\tau^2(p^2+\Delta_0^2) - \Delta_0^2(\cos(2p\tau) + 2p\tau\sin(2p\tau))$.

For the periodic quench model, the expectation values of spin operators at final time $t=T$ under the normalization method are as follows. For $p<0$, $\langle\sigma_z\rangle = 1$, and $\langle\sigma_x\rangle = \langle\sigma_y\rangle = 0$. For $p>0$,

$$\langle\sigma_x(p)\rangle_{\mathrm{norm}} = \frac{4\Delta_0\omega(p^2-\omega^2)}{g_2(p,T)}\sin(pT)\cos(pT), \tag{C2}$$

$$\langle\sigma_y(p)\rangle_{\mathrm{norm}} = \frac{4\Delta_0\omega(p^2-\omega^2)}{g_2(p,T)}\sin^2(pT), \tag{C3}$$

$$\langle\sigma_z(p)\rangle_{\mathrm{norm}} = \frac{4\Delta_0^2\omega^2\sin^2(pT)+(p^2-\omega^2)^2}{4\Delta_0^2\omega^2\sin^2(pT)-(p^2-\omega^2)^2}. \tag{C4}$$

Here, $g_2(p,T) = p^4 - 2\omega^2(p^2-\Delta_0^2) + \omega^4 - \Delta_0^2\omega^2\cos(2pT)$.

Acknowledgements

Project supported by the National Key Research and Development Program of the Ministry of Science and Technology of China (Grant No. 2021YFA1200700), the National Natural Science Foundation of China (Grant Nos. 11905054 and 12275075), and the Fundamental Research Funds for the Central Universities of China.

References

[1] Yoshida T, Peters R and Kawakami N 2018 *Phys. Rev. B* **98** 035141
[2] Shen H and Fu L 2018 *Phys. Rev. Lett.* **121** 026403
[3] Nagai Y, Qi Y, Isobe H, Kozii V and Fu L 2020 *Phys. Rev. Lett.* **125** 227204
[4] Makris K G, El-Ganainy R, Christodoulides D N and Musslimani Z H 2008 *Phys. Rev. Lett.* **100** 103904
[5] Klaiman S, Günther U and Moiseyev N 2008 *Phys. Rev. Lett.* **101** 080402
[6] Malzard S, Poli C and Schomerus H 2015 *Phys. Rev. Lett.* **115** 200402
[7] Rotter I 2009 *J. Phys. A: Math. Theor.* **42** 153001
[8] Mao Y, Zhong P, Lin H, Wang X and Hu S 2024 *Chin. Phys. Lett.* **41** 070301
[9] Hodaei H, Hassan A U, Wittek S, Garcia-Gracia H, El-Ganainy R, Christodoulides D N and Khajavikhan M 2017 *Nature* **548** 187
[10] Bergholtz E J, Budich J C and Kunst F K 2021 *Rev. Mod. Phys.* **93** 015005
[11] Zhang S M, He T Y and Jin L 2024 *Chin. Phys. Lett.* **41** 027201
[12] Zhang K, Yang Z and Fang C 2020 *Phys. Rev. Lett.* **125** 126402
[13] Zhang X J, Zhang T, Lu M H and Chen Y F 2022 *Adv. Phys. X* **7** 2109431
[14] Lamata L, León J, Schätz T and Solano E 2007 *Phys. Rev. Lett.* **98** 253005
[15] Liégeois B, Chitra R and Defenu N 2023 *Phys. Rev. D* **108** 116014
[16] Lee T E 2016 *Phys. Rev. Lett.* **116** 133903
[17] Yao S and Wang Z 2018 *Phys. Rev. Lett.* **121** 086803
[18] Song F, Yao S and Wang Z 2019 *Phys. Rev. Lett.* **123** 246801
[19] Kunst F K, Edvardsson E, Budich J C and Bergholtz E J 2018 *Phys. Rev. Lett.* **121** 026808
[20] Xiong Y 2018 *J. Phys. Commun.* **2** 035043
[21] Jin L and Song Z 2019 *Phys. Rev. B* **99** 081103
[22] Borgnia D S, Kruchkov A J and Slager R J 2020 *Phys. Rev. Lett.* **124** 056802
[23] Xu Z and Chen S 2021 *Phys. Rev. A* **103** 043325
[24] Pan L, Chen X, Chen Y and Zhai H 2020 *Nat. Phys.* **16** 767
[25] Lin Z, Zhang L, Long X, Fan Y a, Li Y, Tang K, Li J, Nie X, Xin T, Liu X J et al. 2022 *npj Quantum Information* **8** 77
[26] Liu H, Yang X, Tang K, Che L, Nie X, Xin T, Li J and Lu D 2023 *Phys. Rev. A* **107** 062608
[27] Kawabata K, Numasawa T and Ryu S 2023 *Phys. Rev. X* **13** 021007
[28] Yoshimura T, Bidzhiev K and Saleur H 2020 *Phys. Rev. B* **102** 125124
[29] McDonald A, Hanai R and Clerk A A 2022 *Phys. Rev. B* **105** 064302
[30] Zhai L J, Huang G Y and Yin S 2022 *Phys. Rev. B* **106** 014204
[31] Das Agarwal K, Konar T K, Lakkaraju L G C and Sen (De) A 2024 *Phys. Rev. A* **110** 012226
[32] Das Agarwal K, Konar T K, Lakkaraju L G C and Sen (De) A 2023 arXiv: 2305.08374v1 [quant-ph]
[33] Matsoukas-Roubeas A S, Roccati F, Cornelius J, Xu Z, Chenu A and del Campo A 2023 *J. High Energy Phys.* **2023** 1
[34] Dong X P, Feng Z B, Lu X J, Li M and Zhao Z Y 2023 *Chin. Phys. B* **32** 034201
[35] Ashida Y, Gong Z and Ueda M 2020 *Adv. Phys.* **69** 249
[36] Turkeshi X and Schiró M 2023 *Phys. Rev. B* **107** L020403
[37] Dóra B, Heyl M and Moessner R 2019 *Nat. Commun.* **10** 2254
[38] Bácsi A and Dóra B 2021 *Phys. Rev. B* **103** 085137
[39] Dóra B, Sticlet D and Moca C P 2022 *Phys. Rev. Lett.* **128** 146804
[40] Dóra B and Moca C P 2020 *Phys. Rev. Lett.* **124** 136802
[41] Longstaff B and Graefe E M 2019 *Phys. Rev. A* **100** 052119
[42] Brody D C 2013 *J. Phys. A: Math. Theor.* **47** 035305
[43] Jing Y, Dong J J, Zhang Y Y and Hu Z X 2024 *Phys. Rev. Lett.* **132** 220402
[44] Mostafazadeh A 2020 *Entropy* **22** 471
[45] Fring A and Moussa M H Y 2016 *Phys. Rev. A* **93** 042114
[46] Mostafazadeh A 2018 *Phys. Rev. D* **98** 046022
[47] Fring A and Moussa M H Y 2016 *Phys. Rev. A* **93** 042114
[48] Fring A and Frith T 2018 *J. Phys. A: Math. Theor.* **51** 265301
[49] Feinberg J and Znojil M 2022 *J. Math. Phys.* **63** 013505
[50] Carmichael H 1993 *An Open Systems Approach to Quantum Optics* (Berlin: Verlag)
[51] Graefe E M, Korsch H J and Niederle A E 2008 *Phys. Rev. Lett.* **101** 150408
[52] Ashida Y and Ueda M 2018 *Phys. Rev. Lett.* **120** 185301
[53] Sim K, Defenu N, Molignini P and Chitra R 2023 *Phys. Rev. Lett.* **131** 156501
[54] Sim K, Defenu N, Molignini P and Chitra R 2025 *Phys. Rev. Res.* **7** 013325